International Journal of Mass Spectrometry 308 (2011) 35–40

Contents lists available at ScienceDirect

International Journal of Mass Spectrometry

journal homepage: www.elsevier.com/locate/ijms

Electron impact total ionization cross sections for H_2S, PH_3, HCHO and HCOOH

Minaxi Vinodkumar[a,*], Harshad Bhutadia[a], Chetan Limbachiya[b], K.N. Joshipura[c]

[a] V.P. & R.P.T.P. Science College, Vallabh Vidyanagar 388 120, India
[b] P.S. Science College, Kadi 382 715, India
[c] Department of Physics, Sardar Patel University, Vallabh Vidyanagar 388120, India

ARTICLE INFO

Article history:
Received 1 April 2011
Received in revised form 12 July 2011
Accepted 12 July 2011
Available online 5 August 2011

PACS:
34.50.−s
34.80.Bm
34.50.Gb

Keywords:
Astrophysical targets
Biological targets
Ionization cross sections
Excitation cross sections
Complex spherical optical potential
Improved complex scattering
potential-ionization contribution

ABSTRACT

This paper reports electron impact total ionization cross sections for molecules H_2S, PH_3, HCHO and HCOOH at energies circa threshold to 2 keV. Spherical Complex Optical Potential (SCOP) is the key ingredient in the Schrodinger equation to generate complex phase shifts and hence the total inelastic cross sections. Total inelastic cross section takes care of total loss of the flux into two dominant channels viz. total electronic excitation (discrete) and total ionization (continuum). We have employed Improved Complex Scattering Potential-ionization contribution (ICSP-ic) a semi empirical method to filter out ionization cross sections from total inelastic cross sections. The results are found to be in overall good agreement with most of the data available in the literature for all the presented targets.

1. Introduction

Ionization is the most fundamental and useful channel of total inelastic processes above the threshold of the target. Ionization and dissociation are the effective tools to probe into structure and dynamics of the target as well as the dominant fragment species produced due to these processes. In fact, in the quantitative study of energy loss of electrons in gases, the total ionization cross sections per unit energy range plays a pivotal role. Ionization cross sections find key place in various applied fields such as upper atmospheric physics, astrophysics, plasma physics, radiation sciences and dosimetry etc. Because of the utility of the total ionization cross sections in various sectors of applied physics there is an ever increasing demand of reliable cross section data.

We discuss briefly the importance of present targets and relevance of the present study. The absolute cross section for both ionization and dissociation process of organic molecules by solar wind are extremely relevant and essential as input for physico-chemical models [1,2]. Interaction of electrons in particular (<20 eV) with biological targets have gained prominence also due to the established fact that secondary electrons produced by highly energetic particles are responsible for single and double strand breaks in DNA [3]. The two present biological targets, HCHO and HCOOH are also important owing to detection of their presence in the dense interstellar clouds [4,5]. Formaldehyde is the first organic molecule detected in space [4] and formic acid is detected in several astronomical sources such as protostellar ices, condritic meteorites, dark molecular clouds and comets [6]. Both these also important targets playing a key role in the chemistry of prebiotic molecules [7] like amino acids which are the primary constituents responsible for origin of life. This shows the relevance and importance of present study for these two species.

Phosphine is dominantly used in the processing of materials utilized for micro and optoelectronics. Phosphine not only serves to be the suitable source of phosphorous dopant for the atomic-scale devices for quantum computing [8] but also has widespread applications in semiconductor industry. Apart from its industrial applications, the study becomes still more important due to its traces found in the lower and upper terrestrial troposphere [9,10]. Finally H_2S is classified as a toxic chemical and is also present in the central star in the "Rotten Egg" nebula and is found in the extragalactic sources. It is one of the species found in Venus atmosphere [11] and has been also detected in comets [12].

* Corresponding author. Fax: +91 2692 235207.
E-mail address: minaxivinod@yahoo.co.in (M. Vinodkumar).

1387-3806/$ – see front matter © 2011 Elsevier B.V. All rights reserved.
doi:10.1016/j.ijms.2011.07.017

Despite the importance of the molecular species studied here, there is scarcity of theoretical as well as experimental data on electron impact total ionization cross sections. Experimental results for formaldehyde are reported by only one group, Vacher et al. (11–85 eV) [13] and theoretical data are reported on NIST website (11–5000 eV) by using BEB formalism [14]. Similarly for formic acid the lone measurements are reported by Pilling et al. (70–2000 eV) [15] and theoretical data are reported by Mozejko (11–4000 eV) using BEB formalism [16]. While no theoretical data for PH_3 is available, experimental data are reported by only Märk and Egger (10.3–183 eV) [17]. In contrast to all other targets studied here, H_2S molecule is more attended experimentally. Theoretical data for H_2S are reported on NIST website calculated by BEB formalism (11–5000 eV) [14] and by Khare and Meath using semi empirical formula [18]. The experimental data are measured by Rao and Srivastava (0–1000 eV) [19], Lindsay et al. (16–1000 eV) [20] and Belic and Kurepa (13–100 eV) [21], while Otvos and Stevenson [22] have reported measured total ionization cross sections at 75 eV.

We report here total ionization cross sections for the targets listed above using Improved Complex Scattering Potential-ionization contribution (ICSP-ic) formalism [23]. The method has been already employed and tested successfully [23]. In the next section we describe the theoretical methodology applied by us to compute total ionization cross sections.

2. Theoretical methodology

The electron atom/molecule scattering phenomenon is characterized quantitatively by two important cross sections viz. total elastic and total inelastic cross sections and they combine to represent total cross sections. Accordingly we have,

$$Q_T(E_i) = Q_{el}(E_i) + Q_{inel}(E_i) \tag{1}$$

where the first term on the right hand side accounts for all elastic processes while the second term takes care of loss of flux in the outgoing channel resulting from electronic excitations and ionization. We are interested here in the total ionization cross sections and hence the second term of Eq. (1) is important. The inelastic processes are taken into account through the complex part of the optical potential via absorption potential. The complete spherical complex optical potential (SCOP) [24] is represented by

$$V_{opt}(E_i, r) = V_R(E_i, r) + iV_I(E_i, r) \tag{2}$$

where, the real part V_R consists of static potential (V_{st}), exchange potential (V_{ex}), and polarization potential (V_p). Owing to the fixed nuclei approximation, the static potential (V_{st}) is calculated at the Hartree-Fock level. The exchange potential (V_{ex}) is responsible for electron exchange between the incoming projectile and the target-electrons. The polarization potential (V_p) combines the short range correlation and long range polarization effect that arises due to the momentary redistribution of target charge cloud which gives rise to dipole and quadrupole moments. The second term of Eq. (2) is the imaginary part of the potential which is taken care by absorption potential. It is to be noted here that the spherical complex optical potential (SCOP) as such does not require any fitting parameters. All the potentials described vide Eq. (2) are charge–density dependent. Hence, representation of target charge density is very crucial. We have employed atomic charge density derived from the Hartree Fock wave functions of Bunge and Barrientos [25]. In order to represent the target molecule we have adopted single centre approach where the charge–density of all constituent atoms is expanded at the centre of mass of the system. The molecular charge density, $\rho(r)$, so obtained is renormalized to incorporate the covalent bonding as described in our earlier paper [26]. In the SCOP [26] formalism, the spherical part of the complex optical potential is used to solve exactly the Schrödinger equation using partial wave analysis to yield various cross sections [24]. Presently our absorption potential is elastic to both vibrational and rotational excitations of the target.

As discussed earlier the absorption potential takes care of loss of flux into all allowed inelastic channels. For this we have used model potential of Staszewska et al. [27] which is non empirical, quasifree, Pauli-blocking and dynamic in nature. The full form of model potential is represented by

$$V_{abs}(r, E_i) = -\rho(r)\sqrt{\frac{T_{loc}}{2}} \times \left(\frac{8\pi}{10k_F^3 E_i}\right) \times \theta(p^2 - k_F^2 - 2\Delta)(A_1 + A_2 + A_3) \tag{3}$$

The parameters A_1, A_2 and A_3 are defined as,

$$A_1 = 5\frac{k_f^3}{2\Delta}; \quad A_2 = \frac{k_f^3(5p^2 - 3k_f^2)}{(p^2 - k_f^2)^2};$$

$$A_3 = \frac{2\theta(2k_f^2 + 2\Delta - p^2)(2k_f^2 + 2\Delta - p^2)^{5/2}}{(p^2 - k_f^2)^2} \tag{4}$$

The local kinetic energy of the incident electron is given by

$$T_{loc} = E_i - (V_{st} + V_{ex}) \tag{5}$$

The dynamic absorption potential is density functional wherein it depends on charge density ($\rho(r)$) of the target, incident energy (E_i) and the parameter Δ of the target. It is sensitive to short range potential like static and exchange through term T_{loc} and insensitive to long range potentials like polarization. In Eq. (3), $p^2 = 2E_i$, represents the momentum transfer of incident electron in Hartree, and $k_F = [3\pi^2\rho(r)]^{1/3}$ is the Fermi wave vector. Also, $\theta(x)$ is the Heaviside unit step-function which depends on p, k_F and Δ, such that $\theta(x) = 1$ for $x \geq 0$, and is zero otherwise. In other words $\theta(x)$ defines the boundary below which the absorption potential is zero and above which it has finite value. The dynamic parameters A_1, A_2 and A_3 of Eq. (3) are the functions of $\rho(r)$, I, Δ and E_i. The parameter Δ is very important since it determines a threshold below which $V_{abs} = 0$, implying that the ionization or excitation channels are prevented energetically. This further infers that the Δ parameter represents the threshold energy for continuum states, which means only ionization process is taken into account, excitation to discrete levels being ignored by the original model [28]. So in order to include the excitations due to discrete levels at lower energy, we have considered Δ as the energy dependent parameter. A variable Δ accounts for more penetration of the absorption potential in the target charge-cloud region [29–32]. Following the earlier works in this regard [29–32], we express Δ as a function of E_i around I as

$$\Delta(E_i) = 0.8I + \beta(E_i - I) \tag{6}$$

Here, β is obtained by requiring that $\Delta = I$ at $E_i = E_p$, where E_p is the value of E_i at which Q_{inel} attains maximum value. For $E_i > E_p$, Δ is held constant equal to ionization energy of the target as suggested in the original model of Staszeweska et al. [27].

After generating the full complex optical potential given in Eq. (2) for a given electron molecule system, we solve the Schrödinger equation numerically with Numerov method using partial wave analysis. At low incident electron energies with short range potentials, only few partial waves are significant for convergence, e.g., at ionization threshold of the target around 5–6 partial waves are sufficient but as the incident energy increases large number of partial waves are needed for convergence. Using these partial waves the complex phase shifts are obtained which are key ingredients to find the relevant cross sections. The phase shifts contains all the information regarding the scattering event.

Total inelastic cross section determined vide Eq. (1) is not a directly measurable quantity and hence also not directly comparable quantity. However, experimentally the total inelastic cross sections can be obtained as the difference between experimental values of grand total cross sections (beam attenuation experiments) and purely elastic cross sections (obtained by integrating differential elastic cross sections). In practice few experimental groups are doing both the measurements simultaneously, and different groups work in different energy regimes and their experimental uncertainties are also different and hence there is difficulty in obtaining total inelastic cross sections from the experiment. But, it is one of the most important quantities as it contains the ionization and electronic excitations which are directly measurable quantities. Thus, we partition the total inelastic cross sections into its two vital components one due to the discrete electronic excitations and other due to the continuum ionization contribution, as,

$$Q_{\text{inel}}(E_i) = \sum Q_{\text{exc}}(E_i) + Q_{\text{ion}}(E_i) \tag{7}$$

Here, first term represents the sum over total excitation cross sections for all accessible electronic discrete transitions, while the second term is the total cross section due to all allowed electronic transitions to continuum, i.e., ionization. In the present range of energies it is the single ionization that dominates in Eq. (7). The discrete transitions arise mainly from the low-lying dipole allowed transitions for which the cross section decreases beyond E_p. By definition,

$$Q_{\text{inel}}(E_i) \geq Q_{\text{ion}}(E_i) \tag{8}$$

This is an important inequality and it forms the basis for ICSP-ic method. ICSP-ic [23] is the improved version of CSP-ic [29,30] which is well established and has been successfully employed for large varieties of targets [29–32]. The detailed discussion for CSP-ic could be found in earlier publications [33,34] and here only important details required for the present study is discussed.

Total ionization cross section may be estimated from total inelastic cross section by defining an energy dependent ratio $R(E_i)$ given by

$$R(E_i) = \frac{Q_{\text{ion}}(E_i)}{Q_{\text{inel}}(E_i)} \tag{9}$$

such that, $0 < R \lesssim 1$.

As total ionization cross section is a continuous function of energy, we can express this ratio also as a continuous function of energy for $E_i > I$, used in earlier studies as [29–32]

$$R(E_i) = 1 - f(U) = 1 - C_1 \left(\frac{C_2}{U + a} + \frac{\ln(U)}{U} \right) \tag{10}$$

where U is the dimensionless variable defined by, $U = E_i/I$.

The reason for adopting such explicit form of $f(U)$ could be visualized as follows. At high energies the total inelastic cross section follows the Born Bethe term according to which the cross sections falls of as $\ln(U)/U$, but at low and intermediate energies they obey $1/E$ form [35]. Accordingly the first term will take care of the cross section behavior at low and intermediate energies while the second term will take care at high energy. The dimentionless parameters C_1, C_2 and 'a' involved in the above equation are deduced by imposing the three conditions on the ratio as discussed below.

$$R(E_i) \begin{cases} = 0 & \text{for } E_i \leq I \\ = R_p & \text{for } E_i = E_p \\ \cong 1 & \text{for } E_i >> E_p \end{cases} \tag{11}$$

The first condition is an exact condition wherein it states that no ionization process is possible below the ionization threshold of the target implying that the value of the ratio must be zero. Coming to the last condition, which physically states that ionization contribution is almost equal to inelastic contribution at very high ($\sim$10 E_p) energies, this is attributed to the fact that at such high energies there are innumerable channels open for the ionization as against very few finite channels for excitation. At such high energies the contribution of excitation is almost negligible. Thus the ratio approaches unity.

Table 1
Properties of target along with values of R_P in the ICSP-ic method.

Target	E_1 (eV) [39,40]	I (eV) [41]	E_P (eV)	R_P
H_2S	6.26	10.45	44	0.53
PH_3	6.42	9.86	48	0.60
HCHO	5.62	10.88	65	0.48
HCOOH	6.25	11.33	65	0.50

The second condition is very crucial and was empirical in nature in CSP-ic method. R_P is the value of R at $E_i = E_P$, and it was observed that at the peak of inelastic cross section the contribution for ionization is about 70–80%. And this argument was supported by many targets studied through CSP-ic. In order to avoid the empirical nature of the CSP-ic formalism and to compute the value of R_p using target properties such as first electronic excitation energy and ionization threshold of the target ICSP-ic method was developed.

We provide here a theoretical computation of R_P [23] using the target properties. For this purpose, we express R_P using Eqs. (7) and (9) as,

$$R_P = \left(1 - \frac{\sum Q_{\text{exc}}}{Q_{\text{inel}}} \right)_{E_i = E_P} \tag{12}$$

It is very clear from the above equation that in order to evaluate R_p we need to compute the values of total excitation and total inelastic cross sections at $E_i = E_P$. Further to compute $(\Sigma Q_{\text{exc}})_{E_i=E_P}$ we need to sum up all the electronic excitation channels from (first excitation) E_1 to the continuum (I) and similarly to compute $(Q_{\text{inel}})_{E_i=E_P}$ we need to sum up all inelastic channels from E_1 to E_p. As the cross sections are continuous function of energy, we can express the ratio R_P as

$$R_P = 1 - \left(\frac{\int_{E_1}^{I} \left(dQ_{\text{exc}}/dE \right) dE}{\int_{E_1}^{E_P} \left(dQ_{\text{inel}}/dE \right) dE} \right) \tag{13}$$

In terms of the dimensionless parameters $U_1 = E_1/I$ and $U_P = E_P/I$, R_P can be also expressed as $1 - f(U_1, U_P)$.

Thus by knowing the energy dependence of the cross sections for the inelastic channel, the integrations of Eq. (13) can easily be done. In general one expects the energy dependence of the cross section as E^{-r} [36–38]. Accordingly,

$$f(U_1, U_P) = \frac{1 - U_1^r}{1 - (U_1/U_P)^r} \tag{14}$$

However, it can be noted that as per Born-Bethe (BB) theory [35], the dominant part of total cross sections show the E_i^{-1} dependence at low and intermediate energy range. Moreover, at the inelastic peak, the inelastic contribution equals the elastic contribution [29] and so it supports E_i^{-1} dependence at $E_i \approx E_P$. It is also seen that this relation with the exponent $r = 1$ holds true for many targets studied earlier [29–32]. Such generalized energy dependence on the cross sections enables us to compute the ratio R_P for any chosen target using Eqs. (13) and (14). The computed values of R_P using Eq. (13) for present targets are listed in Table 1 along with their target properties. The first electronic excitation energies for the present targets are computed using Quantemol-N software which utilizes UK molecular R matrix code [39].

It is found that the computed R_P values in most of the cases studied here lie around 0.5. We employ this new theoretically estimated value of R_P and compute the ionization cross sections for

Table 2
Total ionization cross sections, Q_{ion} (Å^2) for H_2CO, HCOOH, PH_3 and H_2S. Maximum values of the cross section are shown in the bold print.

E_i (eV)	H_2CO	HCOOH	PH_3	H_2S
12	0.06	0.02	0.09	0.08
14	0.26	0.16	0.34	0.31
16	0.55	0.39	0.68	0.61
18	0.88	0.67	1.07	0.94
20	1.24	0.97	1.47	1.28
25	2.08	1.69	2.40	2.05
30	2.74	2.32	3.20	2.66
40	3.54	3.31	4.07	3.38
50	3.92	3.95	4.36	3.70
60	4.07	4.52	**4.45**	3.87
70	4.27	4.83	4.44	**3.92**
80	4.35	4.99	4.37	3.91
90	4.40	5.14	4.30	3.85
100	**4.42**	**5.21**	4.20	3.78
150	4.17	5.13	3.69	3.38
200	3.86	4.87	3.27	3.02
300	3.25	4.30	2.67	2.49
400	2.80	3.79	2.26	2.13
500	2.45	3.37	1.97	1.86
600	2.18	3.03	1.75	1.66
700	1.96	2.74	1.58	1.50
800	1.78	2.50	1.44	1.38
900	1.63	2.30	1.33	1.27
1000	1.50	2.13	1.23	1.18
1500	1.08	1.54	0.91	0.88
2000	0.84	1.19	0.72	0.70
3000	0.63	0.84	0.50	0.50
4000	0.51	0.67	0.40	0.40
5000	0.43	0.53	0.34	0.32

molecular targets listed in Table 2. The results are plotted graphically and compared with the experimental as well as with other model calculations wherever available.

3. Results and discussion

The theoretical approach of SCOP along with the present ICSP-ic method outlined above is employed to determine total inelastic cross sections, Q_{inel} and total ionization cross sections, Q_{ion} along with a useful byproduct of electronic excitations in terms of the summed cross section $\sum Q_{exc}$. In the present paper, we have investigated hydro compounds of varied interest and computed the total ionization cross sections using the newly computed value of R_P vide Eq. (13).

The ionization cross sections are plotted as function of projectile energy for HCHO, HCOOH, PH_3 and H_2S from threshold of the target to 5 keV vide Figs. 1–4, respectively. The numerical values of the total ionization cross section are tabulated in Table 2 for ready reference.

In Fig. 1, we show the comparison of present total ionization cross sections for e–H_2CO scattering with available data. For H_2CO there is scarcity of theoretical and experimental data. There is only one measurement reported by Vacher et al. [13] with experimental uncertainty of 10% above 20 eV and 20% below 20 eV. It can be seen that there is shift in the data of Vacher et al. [13] below 40 eV above which the present data is well within the experimental uncertainty. Theoretical data using BEB method [14] are in good agreement with present results throughout the range except at the peak where the difference is ~6.49%. The present data is lower compared to our earlier work [42] due to difference in R_p value.

In Fig. 2, we present the comparison of present total ionization cross section for e–HCOOH scattering with available data. As mentioned earlier, for this target also there is void for both theoretical and experimental data. The lone measurements are reported by Pilling et al. [15] and theoretical data is reported by Mozejko [16] using BEB method. We have calculated total ionization cross sections using ICSP-ic method as well as using BEB method employing Quantemol software [39]. There is slight variation (<10%) of present data with the experimental data of Pilling et al. [15] and theoretical data of Mozejko [16]. The difference in the two data calculated by Mozejko [16] and by us using BEB formalism may be due to slight difference in input parameters. Present data finds better comparison with available data compared to our earlier work [42]. The reason for difference is twofold, one due to difference in R_P value and other is due to single centre approach employed in present work against the group additivity employed earlier [42].

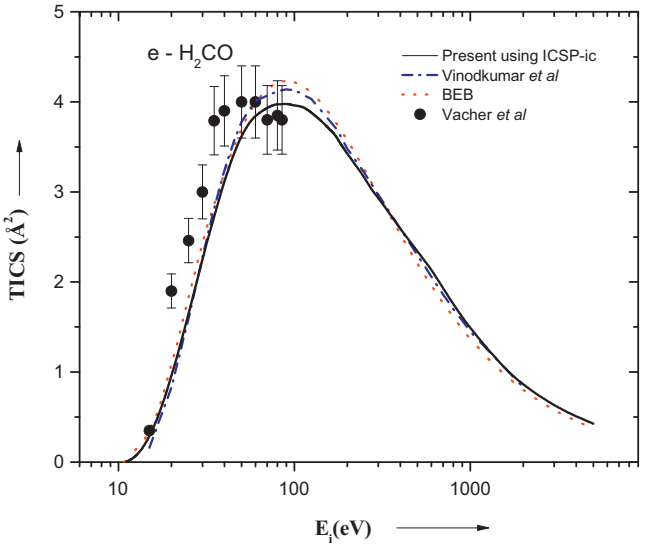

Fig. 1. Total ionization cross sections for e–H_2CO scattering in Å^2. Solid line → present Q_{ion}, dash dot line → Vinodkumar et al. [42], dot line → BEB [14], filled circle → Vacher et al. [13].

Fig. 3 shows the comparison of present total ionization cross section of e–PH_3 scattering with the available theoretical and experimental comparisons. There is paucity of both theoretical and experimental data for this molecule also. There is only one measurement data presented by Märk and Egger [17] with experimental uncertainty of 10%. The present data is overall in very good agreement with experimental data of Märk and Egger [17] and lies well within experimental uncertainty throughout the energy range.

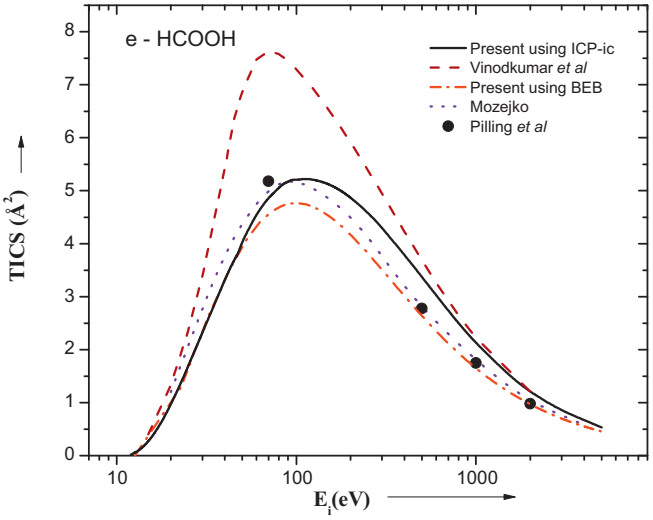

Fig. 2. Total ionization cross sections for e–HCOOH scattering in Å^2. Solid line → present Q_{ion}, dash line → Vinodkumar et al. [42], dash dot line → present result using BEB, dotted line → Mozejko [16], filled square → Pilling et al. [15].

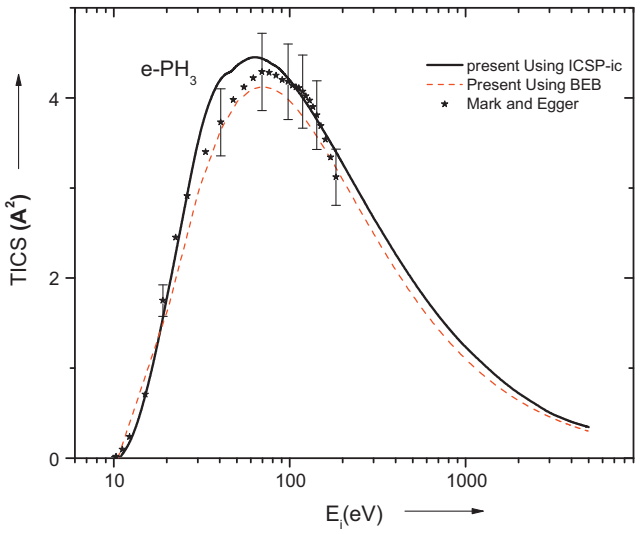

Fig. 3. Total ionization cross sections for e–PH_3 scattering in Å^2. Solid line → present Q_{ion}, dashed line → present result using BEB, filled stars → Märk and Egger [17].

To the best of our knowledge, there is no theoretical data in literature and hence we have calculated total ionization cross sections using ICSP-ic method and BEB formalism. Both theoretical data also show good agreement throughout the energy range except near the peak where they vary by ∼8%.

Finally Fig. 4 shows the comparison of present total ionization cross sections for e–H_2S scattering. The study becomes important as this molecule is investigated by many experimentalist [19–22] and a large variation of about more than 50% is found in the data among different measurements against few theoretical data presented by Kim et al. [14] using BEB formalism and using semi empirical formula by Khare and Meath [18]. Theoretical data of Khare and Meath [18] are not shown in the graph but they are very low and around ∼2 Å^2 at the peak. There is an excellent agreement of present data with theoretical data of Kim et al. [14] throughout the reported energy range except at the peak where there is slight variation. The measured value presented by Otvos and Stevenson [22] is 4.0 Å^2 against present calculated value of 3.9 Å^2 near peak energy 75 eV.

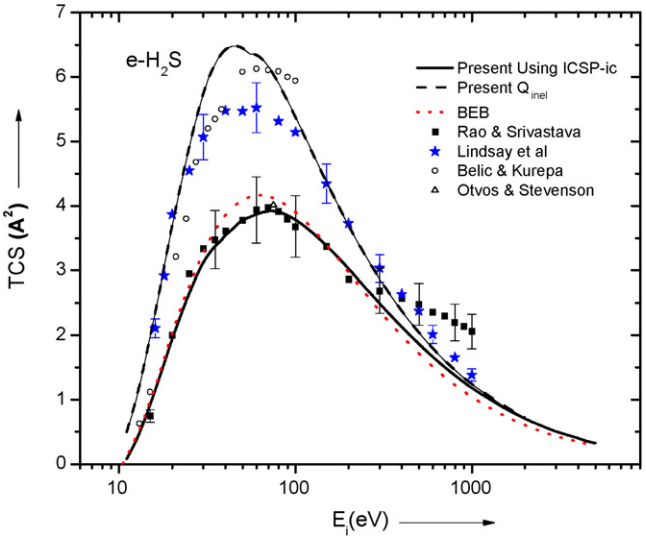

Fig. 4. Total cross sections for e–H_2S scattering in Å^2. Solid line → present Q_{ion}, dash line → present Q_{inel}, dot line → BEB [14], filled square → Rao and Srivastva [19], filled stars → Lindsay et al. [20], open circle → Belic and Kurepa [21], open triangle → Otvos and Stevenson [22].

Measurements of Rao and Srivastava [19] with experimental uncertainty of 13% find very good agreement with present data up to 300 eV. Above 300 eV the data of Rao and Srivastava [19] seems to diverge at high energies compared to all presented results which is regular feature found in their data. The measurements of Lindsay et al. [20] and Belic and Kurepa [21] are exceedingly high at the peak compared to all the theories as well as experiments. The overestimation could be well understood as their data 5.52 Å^2 [20] and 6.13 Å^2 [21] are comparable with present total inelastic cross section (6.35 Å^2) as well as total inelastic cross sections of Jain (6.24 Å^2) [24] at the peak energy of 60 eV. Total ionization cross sections calculated using independent atom model, which generally overestimates at low and intermediate energy turns out to be 5.75 Å^2 which is close to the results of Belic and Kurepa [21] at peak. Thus this also reflects the fact that results of Belic and Kurepa are overestimating. However the peak energy of ionization and shape of the cross section curve is nearly same for all the presented theoretical as well as experimental work.

4. Conclusion

The well established SCOP formalism along with the improved complex scattering potential-ionization contribution (ICSP-ic) formalism is used to derive the total ionization cross section for the present targets HCHO, HCOOH, PH_3 and H_2S. The dynamic ratio, R_P is evaluated using the basic properties of the target such as first electronic excitation energy (E_1) and ionization threshold (I). It is clearly evident from Figs. 1–4 that the present data for the ionization cross sections are in good agreement with available experimental and theoretical data for all the targets studied here. This shows the consistency of the present ICSP-ic formalism and we are now confident to use this method for complex targets as well as targets which are difficult to study experimentally for e.g., exotic targets or radicals. Further, the present method employed here provides an estimate of electronic excitations in relation to ionization cross sections in a particular target. It is to be noted that the present method needs the first electronic excitation energy (E_1) and the ionization threshold (I) as inputs for the calculation of R_p. The present study is significant as the data will be useful to fill the void in the data base and may also inspire the experimentalists for some measurements as these are very important targets.

Acknowledgement

MVK is thankful to DST, New Delhi, for funding Major Research Project and KNJ is thankful to ISRO, Bangalore, for the Major research project, under which part of this work is carried out.

References

[1] S.A. Haider, A. Bhardwaj, Icarus 177 (2005) 196.
[2] S.D. Rodgers, S.B. Charnley, W.F. Huebner, D.C. Boice, in: M.C. Festou, H.U. Keller, H.A. Weaver (Eds.), Comets II, vol. 745, University of Arizona Press, Tucson, 2004, p. 505.
[3] B. Boudaiffa, P. Cloutier, D. Hunting, M.A. Huels, L. Sanche, Science 297 (2000) 1658.
[4] F. Arnold, D. Krankowsky, K.H. Marien, Nature 267 (1977) 30.
[5] P. Ehrenfreund, S.B. Charnley, Ann. Rev. Astron. Astrophys. 38 (2002) 427.
[6] S. Pilling, A.C.F. Santos, H.M. Boechat-Roberty, G.G.B. de Souza, M.M. Sant' Anna, A.L.F. Barros, W. Wolff, N.V. de Castro Faria, Braz. J. Phys. 36 (2B) (2006) 538.
[7] D.E. Woon, APJ 571 (2002) L177.
[8] M.Y. Simmons, S.R. Schofield, J.L. O'Brien, N.J. Curson, L. Oberbeck, T. Hallam, R.G. Clark, Surf. Sci. (2003) 532.
[9] F. Eismann, D. Glindemann, A. Bergmann, P. Kuschk, Chemosphere 35 (1997) 523.
[10] D. Glindemann, M. Edwards, P. Kuschk, Atmos. Environ. 37 (2003) 2429.
[11] J.H. Hoffman, R.R. Hodges, T.M. Donhue, M.B. McElroy, Composition of the Venus lower atmosphere from the pioneer Venus mass spectrometer, J. Geo. Phys. Res. 85 (1980) 7882.

[12] M.L. Marconi, D.S. Mendis, A. Korth, A. Lin, R.P.D.L. Mitchell, H. Reme, The identification of H_3S^+ with the ion of mass per charge (m/q) 35 observed in coma of comet halley, Astrophys. J. 352 (1990) 17.
[13] J.R. Vacher, F. Jorand, N. Blin-Simiand, S. Pasquiers, Chem. Phys. Lett. 476 (2009) 178.
[14] National Institute of Standards and Technology Website: http://physics.nist.gov/PhysRefData/Ionization/molTable.html.
[15] S. Pilling, A.C.F. Santos, W. Wolff, M.M. Sant'Anna, A.L.F. Barros, G.G.B. de Souza, N.V. de castro faria, H.M. Boechat-Roberty, Mon. Not. R. Astron. Soc. 372 (2006) 1379.
[16] P. Mozejko, Eur. Phys. J. Special topics 144 (2007) 233.
[17] T.D. Märk, F.J. Egger, Chem. Phys. 67 (6) (1977) 2629.
[18] S.P. Khare, W.J. Meath, J. Phys. B: At. Mol. Phys. 20 (1987) 2101.
[19] M.V.V.S. Rao, S.K. Srivastava, J. Geophys. Res. 98 (1993) 13137.
[20] B.G. Lindsay, R. Rejoub, R.F. Stebbings, J. Chem. Phys. 118 (2002) 5894.
[21] D.S. Belic, M.V. Kurepa, Fizika 17 (1985) 117.
[22] J.B. Otvos, D.P. Stevenson, J. Am. Chem. Soc. 78 (1956) 546.
[23] M. Vinodkumar, K. Korot, P.C. Vinodkumar, Eur. Phys. J. D59 (2010) 379.
[24] A. Jain, K.L. Baluja, Phys. Rev. A 45 (1) (1992) 202.
[25] C.F. Bunge, J.A. Barrientos, At. Data Nucl. Data Tables 53 (1993) 113.
[26] M. Vinodkumar, K.N. Joshipura, N.J. Mason, Acta Phys. Slov. 56 (4) (2006) 521.
[27] G. Staszewska, D.W. Schwenke, D. Thirumalai, D.G. Truhlar, Phys. Rev. A 28 (1983) 2740.
[28] F. Blanco, G. Garcia, Phys. Rev. A 67 (2003) 022701.
[29] M. Vinodkumar, K. Korot, H. Bhutadia, Int. J. Mass. Spectrom. 294 (2010) 54.
[30] M. Vinodkumar, R. Dave, H. Bhutadia, B.K. Antony, Int. J. Mass. Spectrom. 292 (2010) 7–13.
[31] M. Vinodkumar, K.N. Joshipura, C.G. Limbachiya, B.K. Antony, Atomic Structure and Collision Processes', Narosa Publishing House, 2009, p. 177.
[32] M. Vinodkumar, C. Limbachiya, H. Bhutadia, J. Phys. B. 43 (2010) 015203.
[33] K.N. Joshipura, M. Vinodkumar, C.G. Limbachiya, B.K. Antony, Phys. Rev. A 69 (2004) 022705.
[34] K.N. Joshipura, M. Vinodkumar, B.K. Antony, N.J. Mason, Euro. Phys. J. D23 (2003) 81.
[35] G. Garcia, F. Blanco, Phys. Rev. A 62 (2000) 044702.
[36] G. Garcia, F. Manero, Chem. Phys. Lett. 280 (1997) 419.
[37] A. Zecca, G.P. Karwasz, R.S. Brusa, Phys. Rev. A 46 (1992) 3877.
[38] C. Szmystkowski, A.M. Krzysztofowicz, J. Phys. B: At. Mol. Opt. Phys. 28 (1995) 4291.
[39] J. Tennyson, J. Phys. B: At. Mol. Opt. Phys. 29 (1996) 6185.
[40] C.G. Limbachiya, M. Vinodkumar, N.J. Mason, Phys. Rev. A 83 (2011) 042708.
[41] Available from: http://srdata.nist.gov/cccbdb/.
[42] M. Vinodkumar, K.N. Joshipura, C. Limbachiya, N.J. Mason, Phys. Rev. A 74 (2006) 022721.